Laser and Particle Beams

cambridge.org/lpb

Extreme ultraviolet holography using a laser-plasma source based on xenon/helium gas puff target

P. Wachulak, A. Sarzyński, A. Bartnik, T. Fok and H. Fiedorowicz

Institute of Optoelectronics, Military University of Technology, 2 Kaliskiego Str., 00-908 Warsaw, Poland

Original Study

Cite this article: Wachulak P, Sarzyński A, Bartnik A, Fok T, Fiedorowicz H (2018). Extreme ultraviolet holography using a laser-plasma source based on xenon/helium gas puff target. *Laser and Particle Beams* **36**, 8–14. https://doi.org/10.1017/S0263034617000866

Received: 28 September 2017
Accepted: 14 November 2017

Key words:
Double stream gas puff target; extreme ultraviolet; Gabor holography

Author for correspondence: P. Wachulak, Institute of Optoelectronics, Military University of Technology, 2 Kaliskiego Str., 00-908 Warsaw, Poland. E-mail: wachulak@gmail.com

Abstract

In this paper, we present the application of partially spatially coherent extreme ultraviolet (EUV) radiation from xenon plasma from a laser-plasma source, based on a double stream gas puff target, in coherent imaging. The radiation at the wavelength of 13.5 ± 0.5 nm was employed to record Gabor-type holograms. An iterative algorithm, based on a phase retrieval technique, was developed and used to remove the twin image from the reconstructed EUV image of test objects. Using partially coherent radiation from a compact, laser-plasma source based on a double stream gas puff target, which is intrinsically incoherent, a Gabor EUV holography was successfully demonstrated.

Introduction

Various applications often require both spatially and temporary coherent sources of short wavelength radiation. Coherent diffraction imaging, Chapman *et al.* (2011), holography, Nishino *et al.* (2010), or interferometry, Gorobtsov *et al.* (2017), would not be achievable without the use of coherent photon beams. The state of the art sources of coherent radiation are synchrotrons and Free Electron Lasers, where the pioneering experiments are being performed, however, in the recent years more effort has been devoted to the development of more compact sources of such radiations, such as high order harmonic generation (HHG) sources, Luu and Wörner (2016), laser pumped solid state extreme ultraviolet (EUV), and soft X-ray (SXR) sources, Reagan *et al.* (2014), or capillary discharge lasers, Heinbuch *et al.* (2005). The coherent EUV and SXR radiations are also crucial for important achievements in diffraction imaging, Seaberg *et al.* (2011), high-resolution holography, Wachulak *et al.* (2008), among others.

Various types of targets are employed for generation of the EUV and SXR radiation, including solid and liquid targets, for laser–matter interactions. Among compact EUV and SXR sources, there are also sources that use gas type targets to produce laser plasmas, which emit short wavelength radiation. These sources are often referred to as gas jet sources, Kubiak *et al.* (1998). Derivatives of those are double stream gas puff targets, which inject not one but two gasses into the laser–matter interaction region. While the inner gas is the material of the target, to which a specific elemental emission can be attributed, the second gas surrounds the inner gas decreasing the density gradient of the target gas in the direction of the nozzle axis, increasing target density in the interaction region. Such laser-plasma EUV/SXR source based on a double stream gas puff target was already proven to be useful for various applications, including metrology, Fiedorowicz *et al.* (2005), full-field imaging, Wachulak *et al.* (2013*a*), nanoscale microscopy, Wachulak *et al.* (2015), photoionization, Bartnik *et al.* (2013), spectroscopy, Bartnik *et al.* (2014), polymer surface modification, Bartnik *et al.* (2012), radiobiology, Adjei *et al.* (2015), etc. All those applications were related to the use of spatially incoherent EUV and SXR radiation.

For particular applications, however, such as compact, table top holography, spatially and temporally coherent radiations are required that allow to encode the amplitude and phase of the radiation field emerging from the object. For that compact, coherent sources of EUV and SXR radiation are necessary. The holographic experiments in the EUV and SXR range were successfully performed using HHG sources, Williams *et al.* (2015), or capillary discharge EUV laser in Gabor, Wachulak *et al.* (2007), and Fourier, Malm *et al.* (2013), configurations, however, laser-plasma sources, forming freely expanding spherical in shape plasmas usually emit uniformly into a 4π solid angle and are intrinsically, spatially, and temporally incoherent. Thus, so far, they have been extensively and exclusively used for incoherent applications.

In this work, we would like to show the possibility to perform coherent imaging experiments with such source. We present the results of employing partially coherent EUV emission with usable photon flux from xenon/helium plasma, to perform holography. Gabor in-line holographic scheme was used to record EUV holograms of test objects and the reconstruction

was achieved numerically through back-propagation of the wavefront from the detector plane to the object plane. Additionally, the attempt of suppressing twin image was made, through the use of modified iterative non-linear filtering of a single hologram. In the following sections, the details about this work will be presented and discussed.

Experimental setup

For coherent imaging, a certain degree of spatial and temporal coherence is required. In laser-plasma sources, the plasma is usually not confined in any way, which results in Gaussian-type plasma intensity distribution, Wachulak *et al.* (2013*b*). In our case, the size of the plasma in the EUV spectral region is ~1 mm in diameter, so it can be hardly considered as a point source for applications requiring increased spatial coherence for the experiment. To perform coherent type imaging, using previously mentioned laser-plasma EUV source based on a double stream gas puff target, a partially coherent emission have to be achieved. It is done by spatial and spectral filtering of the quasi-continuous emission from the source.

The experimental setup for the EUV holography using the emission from xenon plasma is depicted in Figure 1a. A Nd:YAG laser beam, emitted from NL 129 laser system (10 J/1–10 ns), from EKSPLA, Lithuania, with laser pulse energy of 4.5 J and 4.3 ns time duration is focused by an $f = 10$ cm focal length lens onto a double stream gas puff target. The target is formed by axisymmetric, collinear, double nozzle, driven separately by two electromagnetic valves. The diameters of the nozzles are 0.4 mm for the inner nozzle and 0.7–1.5 mm for the outer, ring-shaped nozzle. The inner nozzle was pressurized with xenon gas at 8 bar backing pressure, while the outer nozzle was connected to helium pressurized to 6 bars. The double-stream gas puff target was used to increase the gas puff target density, by shaping the flow of the inner gas into a vacuum through the use of the outer gas. In such case higher inner gas density can be obtained at 1.5 mm away from the nozzle to avoid degradation of the nozzle by a repeatable plasma formation. The valves were driven separately by a dedicated two-channel controller, which is capable of independent adjustment of the delay and opening time for each valve. Moreover, driving signals for both valves are synchronized with the laser power supply, which produces a triggering pulse 1 ms before the laser pulse. The delay time and opening times for each valve are 200/750 μs (Xe) and 400/550 μs (He), respectively. More details about the timing and valve synchronization can be found in Wachulak *et al.* (2010). Due to the interaction of the laser pulses with the gaseous target a laser produced plasma is created, which emits radiation in the broad range of wavelengths, from soft X-rays to infrared, depending on the gas used as a target, laser beam and focusing system parameters. In this experiment, an efficient EUV emission was achieved from xenon gas, as was reported by Rakowski *et al.* (2010) and Wachulak *et al.* (2017).

To improve the spatial coherence of the EUV beam, by reducing the apparent source size, a 0.25 mm in diameter pinhole, made by laser drilling in a 100 μm thick steel plate, was introduced 10 mm away from the plasma. This approach, in which high spatial coherence is achieved by spatial filtering at the expense of photon flux, is also very often employed at synchrotron facilities, Attwood (1999). Smaller distance from the pinhole to the plasma causes the thermal damage to the pinhole induced by the plasma. The small inset in Figure 1a shows the SEM micrograph of the pinhole, which is not perfectly round. The major axis D_H was measured to be 251.5 μm, and the minor one

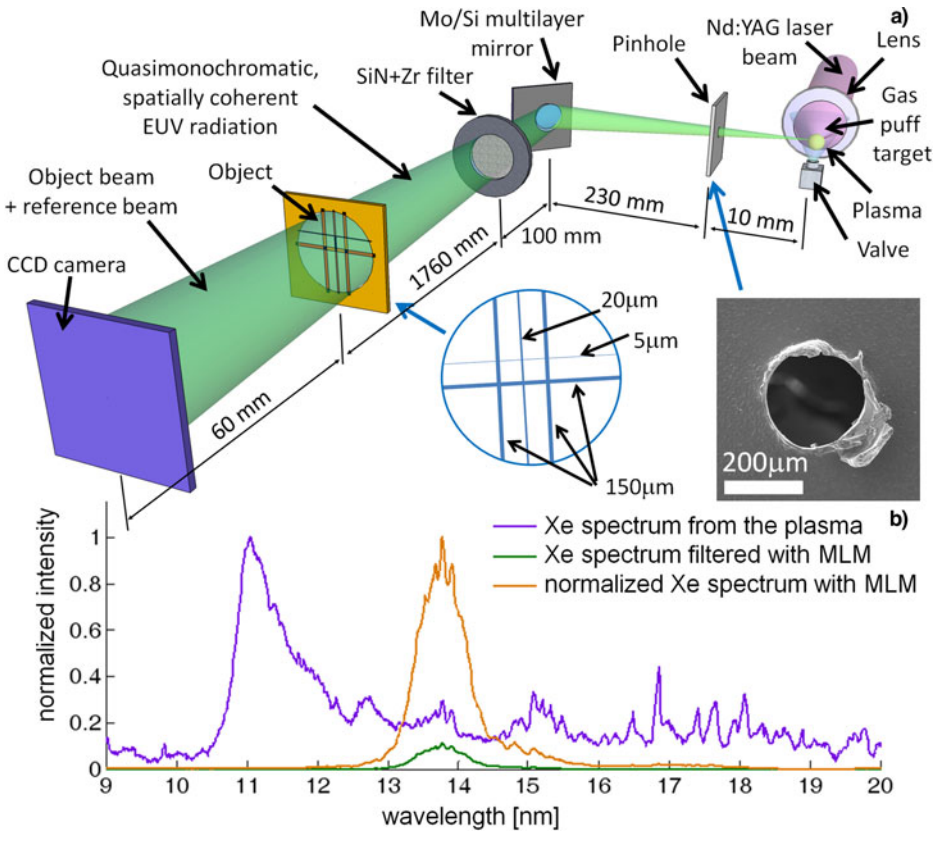

Fig. 1. Schematic description of the experimental setup for EUV holographic imaging employing (a) and the emission spectrum from the Xe/He double stream gas puff target source (b).

https://doi.org/10.1017/S0263034617000866 Published online by Cambridge University Press

$D_V = 234.2$ μm. To monochromatize the EUV beam emitted from the xenon plasma, and in turn, increase the temporal coherence of the source, a Mo/Si multilayer mirror (MLM) was used. The flat mirror was made by depositing Mo/Si multilayers on top of a Si wafer (Jena, Germany). It has a peak reflectivity of 37% for an unpolarized beam at 13.5 nm wavelength, with ±0.5 nm bandwidth and operates at an incidence angle of 45°. A typical spectral emission of the Xe plasma radiation reflected from such mirror in the EUV range from 9 to 20 nm wavelength is depicted in Figure 1b. To remove the visible light emitted from Xe plasma, which is also reflected very efficiently from the MLM, a combined thin film filter (200 nm silicon nitride + 200 nm zirconium) was employed. The object to be imaged was made of different diameter metal wires, from 5 μm in diameter up to 120 μm. It was located at the distance of 2.1 m away from the plasma. The object was entirely illuminated by the partially coherent EUV light, emitted from xenon plasma. The radiation was filtered spatially by the pinhole and spectrally by MLM and set of filters. The hologram, obtained through the interference in the far field between object beam (scattered from the test sample) and the reference beam (from around the object), was recorded by a CCD camera (Andor, DO934N-BN), placed at $z_p = 6$ cm downstream of the object. The camera has a chip with 1024×1024 pixels, each 13×13 μm^2 in size. During the experiments, the chip was cooled down to −20 °C to reduce its internal noise and the background.

Gabor holography with a partially coherent EUV radiation from xenon plasma

To demonstrate the applicability of laser-plasma EUV source based on a double stream gas puff target to imaging a Gabor holography experiments were performed. Since the development of high-resolution cameras, digital holography is applied to many different fields such as microscopy, particle image velocimetry, and deformation analysis. The holography has an important advantage such as the possibility to record not only amplitude of the electric field but also its phase, through the encoding process. Moreover, classical optical reconstruction to recover the information, encoded in the hologram, is nowadays often replaced by the numerical reconstruction, due to its advantages, such as flexibility, accuracy, immunity to the analog reconstruction noises, mechanical vibrations, etc. Additionally, such approach allows for numerical refocusing and reconstruction of 3-D volumes.

In the experiment to record the hologram the object was illuminated by a partially spatially coherent EUV beam with a radius of coherence equal to $R_C = 60$ μm, at the distance of $z_s = 2.1$ m from the source, and with an inverse spectral bandwidth of $\lambda/\Delta\lambda = 14$. The value of the radius of coherence was previously measured using a double-slit Young interferometer with variable slit separation, Wachulak *et al.* (2017), to produce an interference pattern in the far field region. A set of ten slit pairs (the mask), with separations from ∼20 to ∼200 μm, width of each slit ∼4.5–5 μm, and 2.5 mm in length, was fabricated in a 25 μm thick copper foil by repetitive ablation of the material through its interactions with a focused laser beam. The mask was entirely illuminated by the light emitted from xenon plasma and filtered spatially by the pinhole and spectrally by MLM and set of filters. The fringe pattern is formed in the far field, where a charge-coupled device (CCD) camera was located. In an ideal double slit experiment, in which exactly the same two slits are uniformly illuminated, the modulus of the complex coherence factor is equal to the fringe visibility $|\mu_{12}| = V$, Goodman (1985). Thus, it is possible to directly derive information about the spatial coherence of the plasma emission by measurement of the fringe visibility. This was demonstrated in experiments by Thompson and Wolf (1957), with partially coherent visible light and used multiple times to measure the spatial coherence. The visibility of the fringe patterns as a function of the slit separation is depicted in Figure 2. Due to the small difference in the pinhole size between D_H and D_V small changes in the interference pattern visibilities are detectable. This can be seen in Figure 2, in which square markers indicate the visibility values obtained from the intensity profiles for horizontal measurements and circular markers for vertical measurements, respectively. The visibility drops slightly faster in case of horizontal measurements, since $D_H > D_V$. To estimate the radius of coherence of the EUV beam a Gaussian-type function was fitted to the data. The solid line represents the fitted curve for vertical measurements and the dotted line for horizontal measurements. From the data, it was estimated that the radius of coherence in the horizontal direction is equal to $R_{CH} = 56$ μm and in the

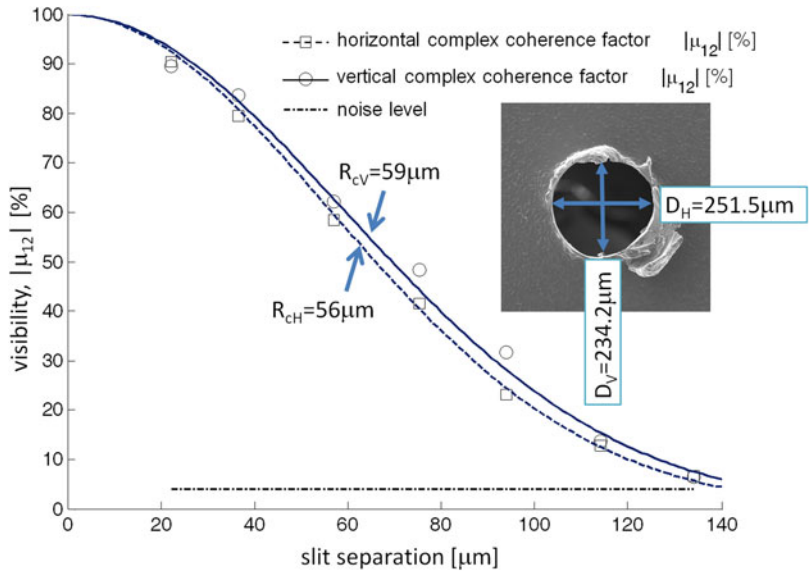

Fig. 2. Visibility, or absolute value of complex coherence factor, as a function of the slit separations for horizontal and vertical measurements. Inset shows the SEM image of the pinhole used for spatial filtering of the Xe plasma EUV radiation. Gaussian profiles were adjusted to fit each set of data, resulting in 56 and 59 μm radii of coherence for horizontal and vertical measurements performed at the distance of 2.1 m from the plasma.

https://doi.org/10.1017/S0263034617000866 Published online by Cambridge University Press

orthogonal direction $R_{CV} = 59$ μm. More details about those measurements, including the discussion about error estimation, can be found in Wachulak *et al.* (2017).

The CCD camera was located at the distance of $z_p = 6$ cm from the object. This caused that the spatial resolution of Gabor hologram was limited theoretically to 3.3 μm by the bandwidth of the EUV emission and to 8.2 μm by the transversal coherence. After the illumination the part of the EUV beam scatters from the object (object beam) and interferes with an un-obscured beam (reference beam) propagating through the openings of the object, producing at the CCD plane an interference pattern. This pattern is a hologram. To obtain a single hologram 30 EUV pulses were used, produced by 5 J energy laser pulses at 10 Hz repetition rate. Example of such hologram is depicted in Figure 3a in the left column. It depicts a representation of the object – crossed wires 150, 20, and 5 μm in diameter. In the zoomed image the 20 and 5-μm wires' edges are surrounded by fringes obtained due to the interference between object and reference beams. Although the diameter of those wires differs by a factor of 4 both wires in the hologram appears to be quite similar in width. The only difference is their "intensity".

The hologram was numerically reconstructed with a Fresnel propagator, Goodman (2005), using an approach similar to Bartels *et al.* (2002) and Wachulak *et al.* (2006). A plane wave was back-propagated by the Fresnel Zone Plate of focal length given by

$$\frac{1}{f} = \frac{1}{z_p} - \frac{1}{z_s + z_p} \tag{1}$$

and rescaled by the geometric magnification equal to $M = (z_s + z_p)/z_s$ of the object, as it is projected onto the CCD camera. The propagation operation was done in the Fourier domain and back-transformed to the spatial domain through equation

$$R(x, y) = \Im^{-1}\{H(f_x, f_y) \cdot F(f_x, f_y)\}, \tag{2}$$

where $R(x, y)$ is the reconstructed image of the object in the spatial domain, $H(f_x, f_y)$ is the hologram in the spatial frequency domain, $F(f_x, f_y)$ is the Fresnel zone plate propagator in the spatial frequency domain and $\Im^{-1}$ denotes inverse 2-D Fourier transform operation. This process has been presented for various reconstruction distances around the value of z_p in Media 1 movie in the Supplementary Materials. In the movie, one can notice how the smallest 5-μm wire reconstructs in and out of focus. The sharpest image is obtained for the reconstruction value equal to z_p. The reconstructed image of the wire objects is depicted in Figure 3a in the right column. Since the object absorbs the EUV light, it appears in the reconstruction as darker than the surrounding area. The zoomed image indicates the 20 μm in

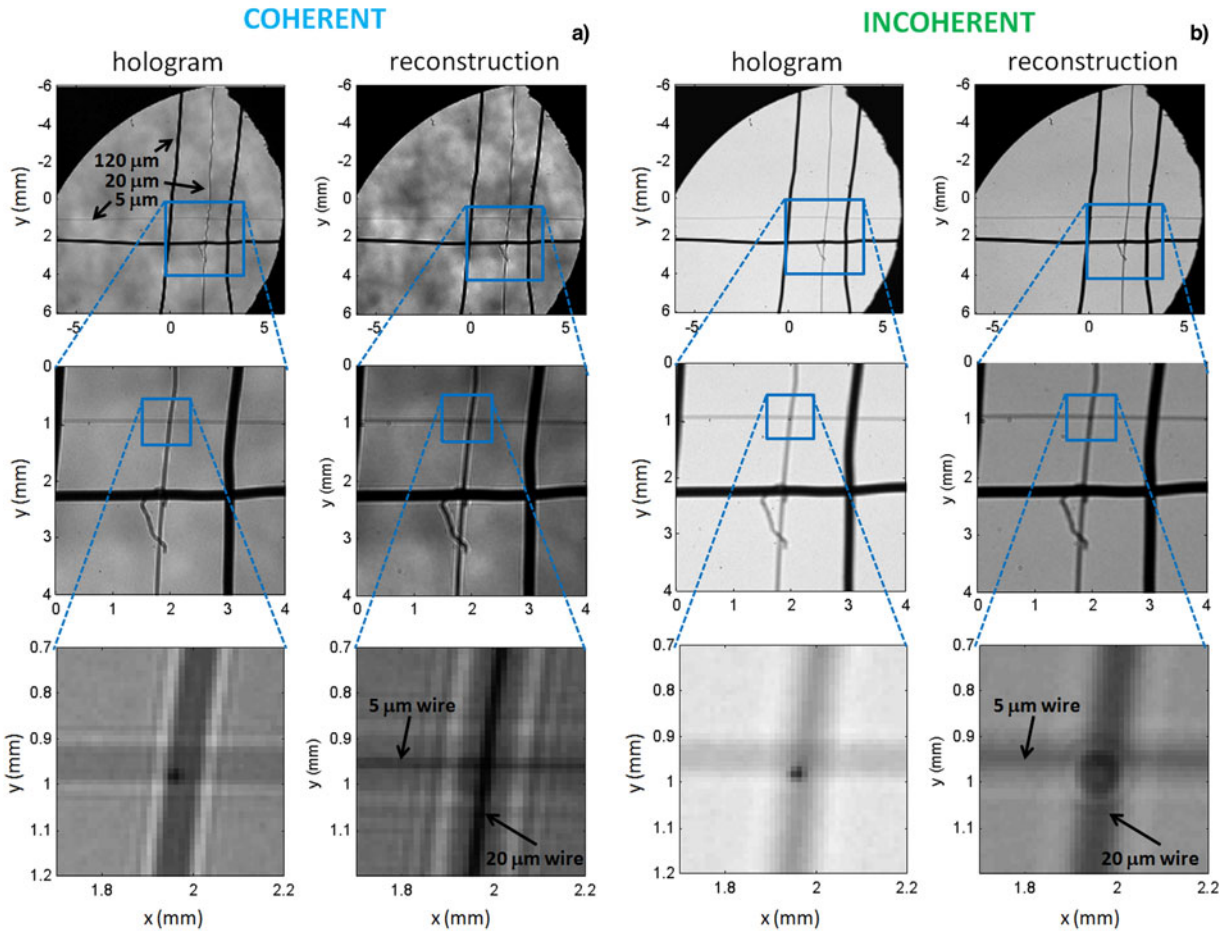

Fig. 3. Gabor-type holograms, obtained using EUV emission from laser-plasma source and numerically reconstructed images of objects – thin wires using spatially coherent EUV radiation (a) and incoherent EUV radiation (b).

https://doi.org/10.1017/S0263034617000866 Published online by Cambridge University Press

diameter wire that was reconstructed properly through the back-propagation algorithm having the size of ~26 μm (two CCD pixels). Taking into account the magnification factor of $M = 1.03$ the diameter of the wire is equal to 25.2 μm, a value, which in good agreement with the real value of 20 μm. Moreover, the 5-μm wire shows the width of ~1–2 pixels in the reconstructed image – a value close to the ultimate resolution in this imaging scheme, equal to the detector's pixel size of 13×13 μm^2. Additionally, after the reconstruction the two wires, being in fact completely opaque at 13.5 nm wavelength, appear, as expected, to have more similar "intensity". The pinhole, used for spatial filtering of the EUV radiation was ~250 μm in diameter. The reconstructed images of wires show that the diameters of the 20 and 5-μm wires are much smaller than the diameter of the pinhole. So the reconstructed image has nothing to do with a simple shadowing effect introduced by the pinhole, which defines the limit of the spatial resolution in classical radiography or shadowgraphy.

To demonstrate further, that spatial coherence is essential for Gabor holography, another hologram was recorded in the exact configuration as previously, with pinhole removed. In that case, the EUV source size was much larger than before (limited by the size of the pinhole). Figure 3b shows the recorded holograms with various zoom factors in the left column and the reconstructed images, obtained through the back-propagation, in the right column. The fringing effect is not present anymore and the reconstruction of the 20 and 5-μm wires is unsuccessful; the reconstructed image is very similar to the hologram, without the possibility to back-propagate the coherent wavefronts to form a sharp reconstruction of the object.

Twin image removal (TIR) from the reconstructed image

While holography in its concept is truly ingenious, even since its invention by Gabor it has been troubled by the so-called twin image problem. The twin image is an artifact, present in the reconstructed image along the reconstructed object, limiting the information that can be obtained from a holographic reconstruction. For the reason of symmetry, there are always two images appearing in the reconstruction of a hologram, namely the reconstructed object and the unwanted out of focus twin image of that object, which obscures the object itself, Latychevskaia and Fink (2007). In this experiment the fringing artifact that can be found in the reconstructions in Figure 3a is attributed to the twin image. There are many possibilities of suppressing the twin image, including the use of a few holograms, recorded at various distances, where two holograms are necessary to suppress the twin-image in an inverse filtering approach, Nugent (1990), or by implementing a phase retrieval procedures to iteratively search for correct, clean and twin-image free phase distribution, Zhang *et al.* (2003).

To suppress the twin image present in Gabor holograms, obtained with Xe/He double stream gas puff target based EUV source, we followed the approach demonstrated by Denis *et al.* (2005). This approach is called iterative non-linear filtering of a single hologram since it requires only one hologram. It is assumed that the signal is in the in-focus real images while the noise is formed by out-of-focus twin-images. However, it should be noted, that the in-focus and out-of-focus images have the same information and are transformed one into another through propagation towards the symmetrical (conjugate) plane with respect to the hologram. Additionally, the objects we are imaging (wires) are located on the same side of the CCD camera. In the algorithm to suppress twin image, the out-of-focus fringes are reduced by masking their focalized counterpart in the virtual image plane, Denis *et al.* (2005).

The flowchart of this approach is presented in Figure 4. The general principle is to clean the twin image fringes by subtracting a correction image *CH*, in a form of complex amplitude, from the hologram *HD*. This complex amplitude is computed through back-propagation of the in-focus virtual objects *RecV* in the virtual image plane. These virtual objects are defined using a constant threshold *th*. The correction image is then applied iteratively to the hologram to achieve twin image cleaning. Contrary to the approach by Denis, who applied the correction image directly to the hologram, we found, that more satisfactory results can be achieved by "gentle" or "soft" suppressing of the twin image. This is done in the final step, before the iteration is completed, by subtracting the properly weighted correction image from the hologram. It is done by multiplying the correction image first by n factor, where $0 < n < 1$. This approach requires a little bit more iterations (e.g. 15 instead of 4–5), however, allows for an additional control over the twin image suppression process.

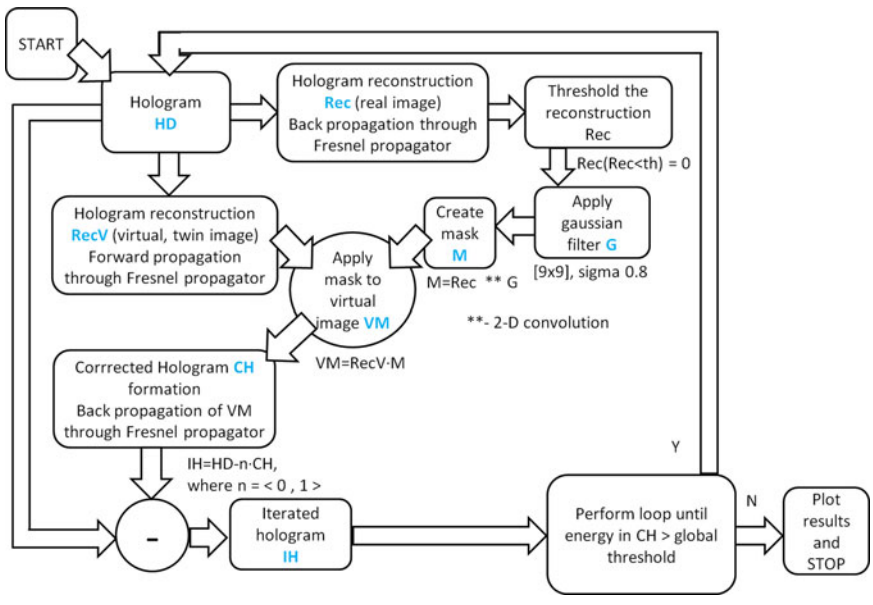

Fig. 4. A "soft" iterative non-linear filtering of a single hologram algorithm used for twin-image removal from reconstructed images of objects obtained from the EUV Gabor holograms. Algorithm modified based on work by Denis *et al.* (2005).

https://doi.org/10.1017/S0263034617000866 Published online by Cambridge University Press

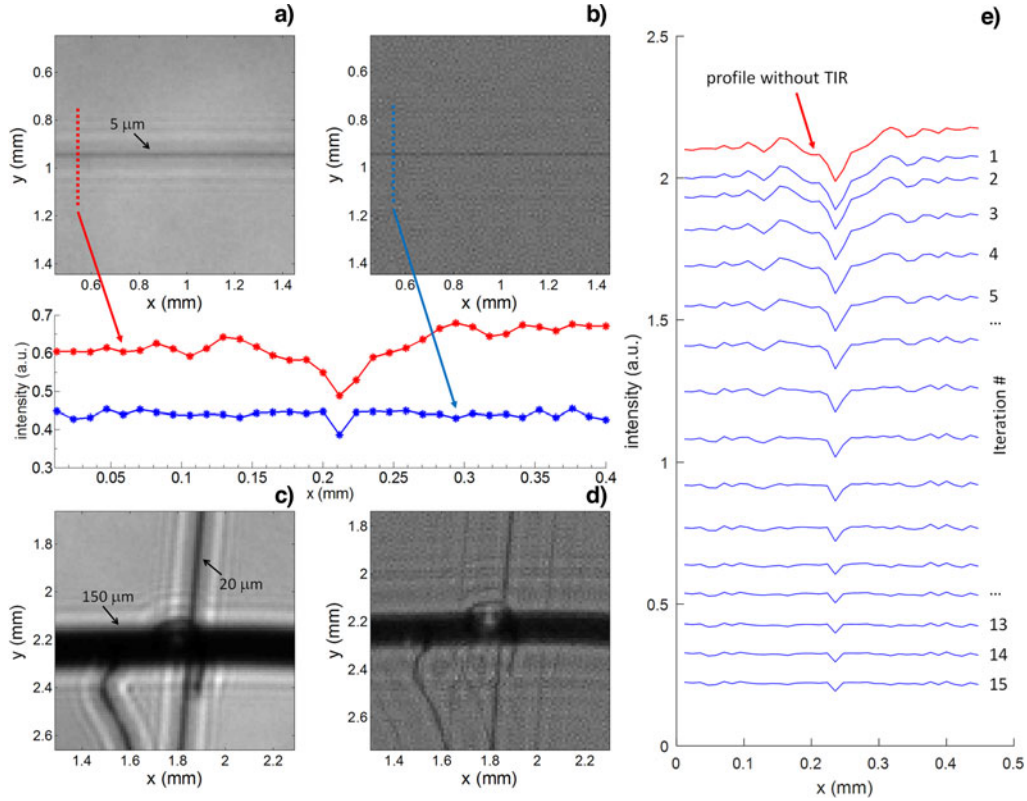

Fig. 5. Reconstructed images of thin wires with twin image artifact present (diffraction effects around the reconstruction) (a, c) and after employing the algorithm depicted in Figure 4, resulting in reducing of the twin image (b, d). Lineouts below images (a) and (b) show the difference in the intensity profiles for reconstructed wires with and without the twin image. After twin image removal it is possible to reconstruct the wire (5 μm wide) with the highest spatial resolution – a single detector pixel ~13 μm in width. Intensity profiles (e) across reconstructed 5-μm wire (red plot) and profiles for each iteration of the twin image removal algorithm (blue plots).

The result of performing TIR from the reconstructions is depicted in Figure 5. The reconstructed EUV image of a 5-μm in diameter wire is presented in Figure 5a. The intensity profile through the reconstructed image is depicted below by a red plot. It clearly shows fringing artifacts present above and below the reconstructed wire. Moreover, the twin image reduces the spatial resolution of the reconstructed image, since the 5 μm in diameter wire appears to be ~2 pixels in width, which is ~26 μm, considering the magnification factor. This value is 3 times larger than the expected theoretical limit, imposed by the partial spatial coherence of the EUV beam to ~8.2 μm. The result of applying the "soft" iterative non-linear filtering of a single hologram algorithm is depicted in Figure 5b. The twin image suppression was achieved with 15 iterations of the code. The representation of the smallest wire is clearly visible as a single, straight darker line and its profile (blue plot) indicate the width of the reconstructed wire to be equal to a single image pixel, equal to ~13 μm. This is equivalent to the ultimate spatial resolution achievable in this type of coherent imaging scheme. The intensity profiles for the reconstructed 5-μm wire for each iteration of the code are depicted in Figure 5e. One can notice that the code converges, resulting in a stable intensity profile for iteration number larger than 10–11 in this case. The result of twin image suppression for each iteration is presented in Media 2 in the Supplementary Materials. Figures 5c and 5d show the result of twin image suppression on the different part of the image. The twin image was partially reduced but still remains, especially for the largest features being 120-μm in diameter wire.

Discussion and conclusions

In the presented work a partially spatially coherent EUV emission from a laser plasma Xe/He double stream gas puff target based source was employed for Gabor holography. The radius of coherence of approximately $R_C = 60$ μm was sufficient to record and reconstruct the holograms with a spatial resolution limited by the pixel size of the detector. Initial reconstruction demonstrated the degrading effect of twin image on the spatial resolution, since the smallest 5-μm in diameter wire appeared to be ~2 pixels in width, equivalent to ~26 μm. This value was approximately 3 times larger than the theoretical limit imposed by a value of the radius of coherence of the EUV beam. Following that, the attempt to suppress the twin image was made through the use of modified iterative non-linear filtering of a single hologram, in which the weighted correction image was applied to the hologram in each iteration step. This procedure allowed obtaining ~2 times better spatial resolution equal to ~13 μm, comparable with the previously mentioned limit, imposed by the partial spatial coherence of the EUV beam of ~8.2 μm.

In conclusion, the xenon laser plasma source based on a double stream gas puff target, which is intrinsically incoherent, can be modified to obtain partial spatial and temporal coherence with the number of coherently emitted EUV photons sufficiently high to perform Gabor in-line holography with spatial resolution comparable with the diffraction limited theoretical value.

Supplementary material. The supplementary material for this article can be found at https://doi.org/10.1017/S0263034617000866.

https://doi.org/10.1017/S0263034617000866 Published online by Cambridge University Press

Acknowledgements. This work is supported by the National Science Centre, Opus programme, grant agreement number UMO-2015/17/B/ST7/03718 and UMO-2015/19/B/ST3/00435 and from the European Union's Horizon 2020 research and innovation program, under Laserlab-Europe IV, grant agreement No. 654148.

References

Adjei D, Getachew Ayele M, Wachulak P, Bartnik A, Wegrzynski Ł, Fiedorowicz H, Vyšín L, Wiechec A, Lekki J, Kwiatek WM, Pina L, Davídková M and Juha L (2015) Development of a compact laser-produced plasma soft X-ray source for radiobiology experiments. *Nuclear Instruments and Methods in Physics Research Section B* **364**, 27–32. doi: 10.1016/j.nimb.2015.08.065.

Attwood DT (1999) *Soft X-rays and Extreme Ultraviolet Radiation*. New York: Cambridge University Press.

Bartels RA, Paul A, Green H, Kapteyn HC, Murnane MM, Backus S, Christov IP, Liu Y, Attwood D and Jacobsen C (2002) Generation of spatially coherent light at extreme ultraviolet wavelengths. *Science* **297**, 376–378.

Bartnik A, Lisowski W, Sobczak J, Wachulak P, Budner B, Korczyc B and Fiedorowicz H (2012) Simultaneous treatment of polymer surface by EUV radiation and ionized nitrogen. *Applied Physics A* **109**(1), 39–43.

Bartnik A, Fedosejevs R, Wachulak P, Fiedorowicz H, Serbanescu C, Saiz EG, Riley D, Toleikis S and Neely D (2013) Photo-ionized neon plasmas induced by radiation pulses of a laser-plasma EUV source and a free electron laser FLASH. *Laser and Particle Beams* **31**(2), 195–201.

Bartnik A, Fiedorowicz H and Wachulak P (2014) Spectral investigations of photoionized plasmas induced in atomic and molecular gases using nanosecond extreme ultraviolet (EUV) pulses. *Physics of Plasmas* **21**(7), 073303.

Chapman HN, Fromme P, Barty A, White TA, Kirian RA, Aquila A, Hunter MS, Schulz J, DePonte DP, Weierstall U, Doak RB, Maia FRNC, Martin AV, Schlichting I, Lomb L, Coppola N, Shoeman RL, Epp SW, Hartmann R, Rolles D, Rudenko A, Foucar L, Kimmel N, Weidenspointner G, Holl P, Liang M, Barthelmess M, Caleman C, Boutet S, Bogan MJ, Krzywinski J, Bostedt C, Bajt S, Gumprecht L, Rudek B, Erk B, Schmidt C, Hömke A, Reich C, Pietschner D, Strüder L, Hauser G, Gorke H, Ullrich J, Herrmann S, Schaller G, Schopper F, Soltau H, Kühnel K, Messerschmidt M, Bozek JD, Hau-Riege SP, Frank M, Hampton CY, Sierra RG, Starodub D, Williams GJ, Hajdu J, Timneanu N, Seibert MM, Andreasson J, Rocker A, Jönsson O, Svenda M, Stern S, Nass K, Andritschke R, Schröter C, Krasniqi F, Bott M, Schmidt KE, Wang X, Grotjohann I, Holton JM, Barends TRM, Neutze R, Marchesini S, Fromme R, Schorb S, Rupp D, Adolph M, Gorkhover T, Andersson I, Hirsemann H, Potdevin G, Graafsma H, Nilsson B and Spence JCH (2011) Femtosecond X-ray protein nanocrystallography. *Nature* **470**(7332), 73–77.

Denis L, Fournier C, Fournel T and Ducottet Ch (2005) Twin-image noise reduction by phase retrieval in in-line digital holography. *Proceedings of SPIE* **5914**, 59140J. doi: 10.1117/12.617405.

Fiedorowicz H, Bartnik A, Jarocki R, Kostecki J, Krzywiński J, Mikołajczyk J, Rakowski R, Szczurek A and Szczurek M (2005) Compact laser plasma EUV source based on a gas puff target for metrology applications. *Journal of Alloys and Compounds* **401**(1–2), 99–103. doi: 10.1016/j.jallcom.2005.02.069.

Goodman JW (1985) *Statistical Optics*. New York: Wiley, pp. 171–187.

Goodman JW (2005) *Introduction to Fourier Optics*. Greenwood Village, CO: Roberts and Company Publishers.

Gorobtsov OYu, Mercurio G, Brenner G, Lorenz U, Gerasimova N, Kurta RP, Hieke F, Skopintsev P, Zaluzhnyy I, Lazarev S, Dzhigaev D, Rose M, Singer A, Wurth W and Vartanyants IA (2017) Statistical properties of a free-electron laser revealed by Hanbury Brown–Twiss interferometry. *Physical Review A* **95**, 023843.

Heinbuch S, Grisham M, Martz D and Rocca JJ (2005) Demonstration of a desk-top size high repetition rate soft x-ray laser. *Optics Express* **13**(11), 4050–4055. doi: 10.1364/OPEX.13.004050.

Kubiak GD, Bernardez LJ and Krenz KD (1998) High-power extreme-ultraviolet source based on gas jets. *Proceedings of SPIE* **3331**, 81. doi: 10.1117/12.309560.

Latychevskaia T and Fink HW (2007) Solution to the twin image problem in holography. *Physical Review Letters* **98**, 233901. doi: 10.1103/PHYSREVLETT.98.233901.

Luu TT and Wörner HJ (2016) High-order harmonic generation in solids: a unifying approach. *Physical Review B* **94**, 115164.

Malm EB, Monserud NC, Brown CG, Wachulak PW, Xu H, Balakrishnan G, Chao W, Anderson E and Marconi MC (2013) Tabletop single-shot extreme ultraviolet Fourier transform holography of an extended object. *Optics Express* **21**(8), 9959–9966.

Nishino Y, Tanaka Y, Okada M, Okaya M, Uozaki Y, Nozaki K, Yabashi M, Nagasono M, Tono K and Kimura H (2010) Femtosecond snapshot holography with extended reference using extreme ultraviolet free-electron laser. *Applied Physics Express* **3**(10), 102701-1–3.

Nugent KA (1990) Twin-image elimination in Gabor holography. *Optics Communications* **78**, 293–299.

Rakowski R, Bartnik A, Fiedorowicz H, de Gaufridy de Dortan F, Jarocki R, Kostecki J, Mikołajczyk J, Ryć L, Szczurek M and Wachulak P (2010) Characterization and optimization of the laser-produced plasma EUV source at 13.5 nm based on a double-stream Xe/He gas puff target. *Applied Physics B* **101**(4), 773–789.

Reagan BA, Berrill M, Wernsing KA, Baumgarten C, Woolston M and Rocca JJ (2014) High-average-power, 100-Hz-repetition-rate, tabletop soft-x-ray lasers at sub-15-nm wavelengths. *Physical Review A* **89**, 053820. doi: 10.1103/PhysRevA.89.053820.

Seaberg MD, Adams DE, Townsend EL, Raymondson DA, Schlotter WF, Liu Y, Menoni CS, Rong L, Chen C, Miao J, Kapteyn HC and Murnane MM (2011) Ultrahigh 22 nm resolution coherent diffractive imaging using a desktop 13 nm high harmonic source. *Optics Express* **19**(23), 22470.

Thompson BJ and Wolf E (1957) Two-beam interference with partially coherent light. *Journal of the Optical Society of America* **47**, 895.

Wachulak P, Sarzyński A, Bartnik A, Fok T, Węgrzynski Ł, Kostecki J and Fiedorowicz H (2017) Spatial coherence measurements of the EUV emission from laser-plasma source based on xenon/helium gas puff target. *Applied Physics B* **123**, 216. doi: 10.1007s00340-017-6795-7.

Wachulak PW, Bartels RA, Marconi MC, Menoni CS, Rocca JJ, Lu Y and Parkinson B (2006) Sub 400 nm spatial resolution extreme ultraviolet holography with a table top laser. *Optics Express* **14**(21), 9636.

Wachulak PW, Marconi MC, Bartels RA, Menoni CS and Rocca JJ (2007) Volume extreme ultraviolet holographic imaging with numerical optical sectioning. *Optics Express* **15**, 10622–10628.

Wachulak PW, Marconi MC, Bartels R, Menoni CS and Rocca JJ (2008) Soft X-ray holography with wavelength resolution. *Journal of the Optical Society of America B* **25**(11), 1811–1814.

Wachulak PW, Bartnik A, Fiedorowicz H, Feigl T, Jarocki R, Kostecki J, Rakowski R, Rudawski P, Sawicka M, Szczurek M, Szczurek A and Zawadzki Z (2010) A compact, quasi-monochromatic laser-plasma EUV source based on a double-stream gas-puff target at 13.8 nm wavelength. *Applied Physics B* **100**(3), 461–469.

Wachulak PW, Bartnik A, Wegrzynski L, Kostecki J, Jarocki R, Fok T, Szczurek M and Fiedorowicz H (2013a) Sub 1-μm resolution "water-window" microscopy using a compact, laser-plasma SXR source based on a double stream gas-puff target. *Nuclear Instruments and Methods in Physics Research Section B* **311**, 42–46.

Wachulak PW, Bartnik A, Skorupka M, Kostecki J, Jarocki R, Szczurek M, Wegrzynski L, Fok T and Fiedorowicz H (2013b) Water-window microscopy using a compact, laser-plasma SXR source based on a double-stream gas-puff target. *Applied Physics B* **111**(2), 239–247.

Wachulak PW, Torrisi A, Bartnik A, Adjei D, Kostecki J, Wegrzynski L, Jarocki R, Szczurek M and Fiedorowicz H (2015) Desktop water window microscope using a double-stream gas puff target source. *Applied Physics B* **118**(4), 573–578. doi: 10.1007/s00340-015-6044-x.

Williams GO, Gonzalez AI, Künzel S, Li L, Lozano M, Oliva E, Iwan B, Daboussi S, Boutu W, Merdji H, Fajardo M and Zeitoun Ph (2015) Fourier transform holography with high harmonic spectra for attosecond imaging applications. *Optics Letters* **40**(13), 3205–3208. doi: 10.1364/OL.40.003205.

Zhang Y, Pedrini G, Osten W and Tiziani HJ (2003) Whole optical wave field reconstruction from double or multi in-line holograms by phase retrieval algorithm. *Optics Express* **11**(24), 3234.